Title: The Effect of the Degree of Premixedness on Self-Excited Combustion Instability

Authors: Adam Howie, Daniel Doleiden, Stephen Peluso, Jacqueline O'Connor

Affiliation: Pennsylvania State University, University Park, PA, USA

ABSTRACT

The use of lean, premixed fuel and air mixtures is a common strategy to reduce NO_x emissions in gas turbine combustors. However, this strategy causes an increased susceptibility to self-excited instability, which manifests as fluctuations in heat release rate, flow velocity, and combustor acoustics that oscillate in-phase in a feedback loop. This study considers the effect of the level of premixedness on the self-excited instability in a single-nozzle combustor. In this system, the fuel can be injected inside the nozzle to create a partially-premixed mixture or far upstream to create a fully-premixed mixture, varying the level of premixedness of the fuel and air entering the combustor. When global equivalence ratio is held constant, the cases with higher levels of premixing have higher instability amplitudes. High-speed CH* chemiluminescence imaging shows that the flame for these cases is more compact and the distribution of the heat release rate oscillations is more concentrated near the corner of the combustor in the outer recirculation zones. Rayleigh index images, which are a metric for quantifying the relative phase of pressure and heat release rate oscillations, suggest that vortex rollup in the corner region is primarily responsible for determining instability characteristics when premixedness is varied. This finding is further supported through analysis of local flame edge dynamics.

Journal of Engineering for Gas Turbines and Power. Received August 27, 2020;
Accepted manuscript posted January 4, 2021. doi:10.1115/1.4049486

NOMENCLATURE

L'	Instantaneous flame edge location oscillation
P'	Pressure fluctuation [Pa]
RMS	Root mean square
$\tilde{p}$	Degree of premixedness
q'	Heat release fluctuation
ϕ_{FPM}	Equivalence ratio of fully premixed fuel and air
ϕ_G	Global equivalence ratio
$\Delta\varphi$	Phase offset between left and right branches

INTRODUCTION

Many modern gas turbine combustor designs use lean premixed combustion to reduce NO_x emissions in compliance with criteria pollutant regulations. One potential drawback of these lean premixed systems is their increased susceptibility to self-excited thermoacoustic instabilities. Instabilities occur when a coupling between combustor acoustics and flame heat release rate oscillations create a positive feedback loop in the system [1]. This feedback is typically driven by intermediary coupling mechanisms, including flow field oscillations and equivalence ratio oscillations. Thermoacoustic instability is undesirable because it reduces combustor efficiency, increases emissions, accelerates component wear, and may result in complete hardware failure [2]. Many studies have investigated the mechanisms that govern both the excitation and damping of thermoacoustic oscillations. Combustor conditions such as inlet velocity [3], swirl intensity [4],

combustor geometry [5, 6], and equivalence ratio [7–9] have been analyzed for their effect on instability in lean premixed systems.

One common way to passively reduce instabilities is through the uneven distribution of the fuel in a combustor with multiple nozzles or multiple fuel circuits in one nozzle; this process is called fuel staging. Fuel staging has been applied to multi-nozzle can combustors by varying the amount of fuel delivered to each nozzle and has been shown to be effective at reducing combustion instability [10–13]. Samarasinghe *et al.* [10] found that staging the center nozzle of a multi-nozzle can combustor causes a redistribution of heat release in the flame and a shift in the phase between pressure and heat release fluctuations. The flame and pressure oscillations become out of phase with each other as a result of the fuel staging, resulting in thermoacoustic damping that reduces the instability amplitude. Culler *et al.* [11] studied the effect of transient fuel staging on the self-excited instability in a multi-nozzle combustor by varying the staging amplitude, duration, and direction of the transient event. This study showed that the transient timescale only depended on the staging amplitude during short transients, and that the timescales associated with the onset of instability are longer and vary more than those associated with decay. In another study performed on the same combustor, Culler *et al.* [12] also investigated the effectiveness of staging a multi-nozzle combustor non-axisymmetrically by comparing the effects of staging an outer nozzle vs. staging the center nozzle. This study showed that staging the outer nozzles is as effective as center nozzle staging, but also demonstrated that slight variations in hardware can have significant and unpredictable effects on the efficacy of fuel staging in any combustor design. Fuel staging has also been found to be effective at suppressing instability in annular combustors [14–17], but the mechanism by which this occurs is likely very different than in a can combustor both because of

the dominant mode of the acoustic oscillation (longitudinal vs. transverse) and the interaction mechanisms between flames.

Most studies of combustion instability use a single nozzle to minimize confounding variables, but most practical combustor designs use multi-nozzle configurations [18–22]. In a study of single-nozzle combustors, Lieuwen *et al.* [23] found a coupling between localized fluctuations in pressure, flow velocity, equivalence ratio, and reaction rate that would excite instability. It was proposed in this study that passive methods of instability suppression may not be equally effective in single-nozzle vs. multi-nozzle combustors due to practical design restrictions.

A small number of studies have compared the conditions in single- and multi-nozzle combustors [24–26]. Fanaca *et al.* [27] investigated the differences in the flame structure between an annular twelve-nozzle combustor and a single nozzle configuration of the same hardware. Similarly, experiments by Szedlmayer *et al.* [28] compared the flame response of five-nozzle can combustor to a comparable single nozzle design. Although these studies were performed on different hardware, both demonstrated that any similarity between single- and multi-nozzle designs is largely dependent on the geometry of the combustor. Smith *et al.* [28,29] showed that there are several key similarities in the unstable flow structures of single- and triple-nozzle flames when subjected to transverse acoustic forcing. This finding provides evidence for the utility of single-nozzle combustion experiments in determining the dynamics of flames in comparable multi-nozzle designs.

Recent work by Chen *et al.* [24] studied the effect of equivalence ratio transients on combustion instability for both single- and multi-nozzle configurations, showing that the confinement from the combustor wall and the interactions between adjacent flames were the greatest factors determining the dynamics of the flame; these results corroborate the work by

Fanaca *et al.* [27] in a different configuration. In this study, a single-nozzle combustor was used to mimic the transient behavior of the outer nozzles of the multi-nozzle combustor as the boundary conditions were most similar; the center nozzle of the multi-nozzle combustor is subjected to a highly irregular flow field and has no flame-wall interaction, resulting in an almost square-shaped flame [31]. Small changes in equivalence ratio were executed in a transient manner and the behavior of the flame during this transient was compared between the single- and multi-nozzle configurations, showing that the mechanism of instability between the outer nozzle and the single nozzle cases were relatively similar, although some of the transient behavior differed. This finding has many similarities with those previously mentioned and begins to bridge the gap in models of instability for single- and multi-nozzle combustors.

The current work follows that of Chen et al. [21,23] and addresses the issue of premixedness and its effect on self-excited instability amplitude. In previous experiments, the variations in equivalence ratio were achieved by adding fuel to the mixture using the fuel circuit inside the nozzle, whereas most of the fuel was fully premixed far upstream of the premixing hardware. Further investigation of this data showed that the instability amplitude at a global equivalence ratio of 0.7 was different depending on the fuel split between the fully-premixed and the partially-premixed fuel delivery circuits.

The degree of premixedness in many gas turbine combustors, described in this paper as "fully," "partially," or "non-premixed," is often decided by the upstream location of fuel injection into the inlet air [32]. Kypraiou *et al.* [33] studied the effect of the level of premixing on the response of flames to acoustic forcing. The results of this experiment showed that partially premixed flames had a higher response to acoustic forcing than both the non-premixed and fully premixed cases and that the mechanisms governing instability were different between non-

premixed and premixed configurations. In another study, Kypraiou *et al.* [34] also compared the dynamics of non-premixed and partially premixed flames near the lean blow-off limit and found that premixing had a marked effect on the forced response under these conditions. Kypraiou's findings are significant in that they demonstrate the ability of premixing to alter the nature of instability in gas turbine combustors. However, it is difficult to make any generalized conclusions based on this due to the lack of consistency in the degree of premixedness from combustor to combustor.

In this work, the effect of the level of premixing on the self-excited thermoacoustic instability is analyzed to identify the reasons why the instability amplitude varies with premixing when the global equivalence ratio is held constant. Instability amplitude, as well as the flame structure and heat release rate fluctuations, are compared for varying degrees of premixedness in a single nozzle combustor to further characterize the mechanisms governing instability.

EXPERIMENTAL METHODS

Experimental Overview

Transient tests are performed on a four-around-one, multi-nozzle, laboratory-scale combustor modified for single-nozzle use in a manner described by Chen *et al.* [24]. The combustor, shown in Figure 1, is fueled by natural gas and air. Optical accessibility to the flame is provided by a quartz liner that measures 305 mm in length and 110 mm in diameter. The nozzle is 55 mm in diameter and uses a swirling annular jet to stabilize the flame. The dump ratio of this configuration was chosen to match that of the multi-nozzle configuration in this same facility [35]. Studies of the effect of dump ratio were previously conducted in this facility [5]; a single dump ratio is used in this study. In the fully-premixed configuration, fuel and air are mixed after a choke

Journal of Engineering for Gas Turbines and Power. Received August 27, 2020;
Accepted manuscript posted January 4, 2021. doi:10.1115/1.4049486

plate upstream of the manifold such that the mixture is considered fully premixed by the time it reaches the inlet nozzle.

Chen *et al*. [24] found that thermoacoustic instability self-excites in this single-nozzle combustor at a global equivalence ratio of 0.7 and higher. In the present analysis, equivalence ratio transients are performed to transition between stable and unstable combustor operation. Instability is excited by injecting additional fuel 0.1 m upstream of the combustor inlet through the fuel staging annulus shown in Figure 1. Transient tests capturing the onset of instability have the global equivalence ratio increased to the unstable value of 0.7 with the addition of staging fuel. Instability decay is achieved when the additional staging fuel is removed from the system. Previous studies using comparable experimental hardware assumed that the staging fuel could fully premix with the main fuel and air based on acetone-PLIF imaging of the partially-premixed fuel and air mixing in the same hardware [32]. However, in this study, mixtures with staging fuel present are considered only partially premixed due to the relatively close upstream location of the staging fuel injection to the inlet nozzle in the combustor design.

Journal of Engineering for Gas Turbines and Power. Received August 27, 2020;
Accepted manuscript posted January 4, 2021. doi:10.1115/1.4049486

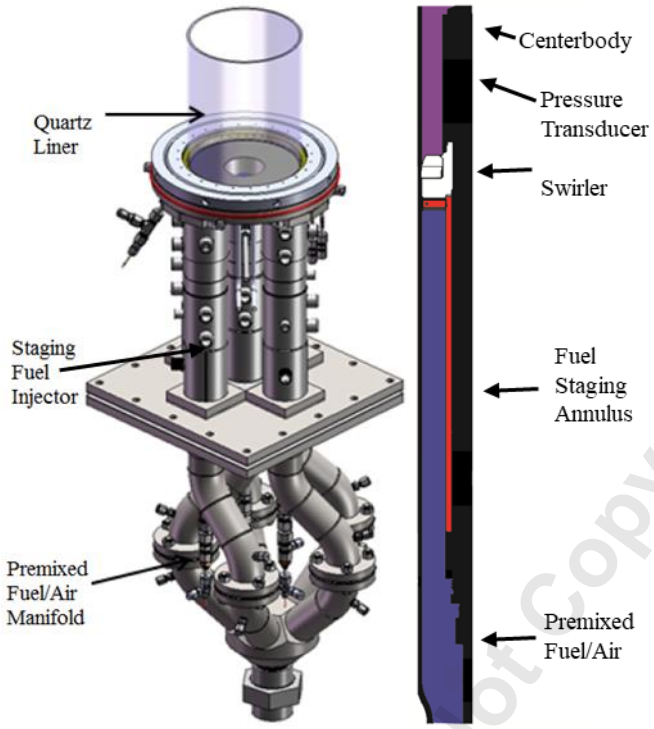

(a) **(b)**

Figure 1: (a) Combustor configuration; (b) Diagram of nozzle inlet geometry including location of pressure port and staging fuel injection

Repeatability of the transient staging process is ensured by controlling the operation, timing, and temperatures of the experiment during each run. All transient tests begin at a baseline condition where there is no self-excited instability and all nozzles are fueled equally with an equivalence ratio of 0.65. The centerbody and dump plane temperatures are recorded at this condition; these temperatures serve as the baseline temperatures that are used as metrics for ensuring repeatability of subsequent tests. Next, the equivalence ratio of all nozzles is increased to 0.70 and the combustor undergoes self-excited oscillations. The transient test is then run. For the instability decay (unstable-to-stable) schedule, the combustor remains unstable for 4 or 8 seconds before the fuel staging is applied. For the instability onset transient (stable-to-unstable), fuel staging is applied immediately and maintained for 4 or 8 seconds after which the valve is closed. After the transient test is completed, the apparatus is brought down to a lower equivalence ratio between 0.50 and

0.55 and allowed to cool below the baseline temperatures between tests. The process described above is one transient ensemble and is repeated for each test. This method of operation helps to ensure that each test condition has the same initial thermal conditions.

This work defines the degree of premixedness as the ratio of the partially premixed staging fuel to the fully premixed main fuel/air at a constant global equivalence ratio as described in Equation (1). Quantification of premixing levels has been performed by Orwannukul [32] using an acetone laser-induced fluorescence, but this technique was not repeated in this study due to hardware limitations. Instead, the qualitative term "premixedness" will be used to compare test cases.

$$\text{“Premixedness"} = \tilde{p} = \phi_{FPM}/\phi_G \quad (1)$$

The test matrix in Table 1 is comprised of three cases that achieve the unstable global equivalence ratio of 0.7 with varying degrees of premixedness. Aside from the source of the fuel, all test cases had the same inlet conditions during unstable operation, which are listed in

Table 2. Uncertainty in equivalence ratio, determined in previous studies [11], is 0.01, which indicates that the fully premixed equivalence ratios are statistically significantly different.

Table 1: Test matrix

ϕ_{FPM}	ϕ_G	$\tilde{p}$
0.625	0.7	0.90
0.65	0.7	0.93
0.675	0.7	0.96

Journal of Engineering for Gas Turbines and Power. Received August 27, 2020;
Accepted manuscript posted January 4, 2021. doi:10.1115/1.4049486

Table 2: Inlet flow conditions

Parameter	Value
Fuel Flow Rate (g/s)	1.16
Air Flow Rate (g/s)	28.52
Inlet Flow Velocity (m/s)	26
Inlet Air Temperature (°C)	200
Inlet Reynolds Number	17,000
Nozzle Swirl Number	0.7

Diagnostics

Pressure fluctuations are measured at 16,384 Hz by a recess mounted PCB dynamic pressure transducer mounted on the nozzle wall 50 mm upstream of the dump plane. It is assumed that there is a continuous propagation of the plane-wave across the nozzle inlet allowing for the correction of measured pressure fluctuations to obtain dump plate pressure [36]. The correction method was validated in the multi-nozzle combustor configuration where both the nozzle and dump-plane pressure transducers are present. The pressure readings are high-pass filtered above 10 Hz to remove low-frequency DC coupling noise in the signal. The instability amplitude for each test case is characterized by the root-mean-square (RMS) of the pressure fluctuations. For a condition to be unstable, the pressure fluctuation RMS must be greater than 500 Pa, or 0.5% of the time-averaged combustor pressure. Additionally, the signal to noise ratio of the instability peak in the pressure spectrum must be greater than 30, ensuring that the instability is tonal.

A K-type thermocouple records the temperature of the tip of the centerbody, which is located 15 mm upstream from the dump plane and is where the flame stabilizes. Another K-type thermocouple is located approximately 1 m upstream of the dump plane and measures the inlet air temperature; a process heater uses this temperature in a feedback loop to ensure constant temperature control throughout the experiments.

CH* chemiluminescence images are taken by a Photron SA4 high speed camera fitted with an Invisible Vision UVi 1850-10 intensifier, a Nikon AF Micro-Nikkor 60mm f/208 lens, and a 432±5 nm bandpass filter. 8000 images are taken at a rate of 4000 frames/second for a frequency resolution of 0.5 Hz. In this study, CH* is used as a marker of combustion activity by assuming a linear dependence of CH* chemiluminescence intensity and heat release rate [31].

Additional high-speed imaging of the flame is taken with planar laser-induced fluorescence of OH (OH-PLIF) at a rate of 10,000 frames/second. The OH-PLIF system consists of a 532 nm Nd:YAG laser (Edgewave) pumping a dye laser (Sirah Credo). The output beam is tuned to the Q1(6) line of the $A^2\Sigma^+ \leftarrow X^2\Pi$ (1-0) band to excite the OH radicals at 282.94 nm. The signal from the excited OH radicals is acquired using a CMOS sensor camera (Photron FASTCAM SA1.1), coupled with an external intensifier (LaVision HS-IRO) and a 100 mm f/2.8 UV lens (Cerco). A high transmissivity filter (LaVision 1108760 VZ) is used to collect the signal at 320±20 nm. Background flame luminosity is reduced in the acquired images by setting the intensifier gate at 100-150 ns. OH-PLIF has been used to investigate both forced and unforced turbulent flame-flame interactions [34,35] and study the instantaneous flame dynamics of lean premixed swirl stabilized flames in a multi-nozzle combustor [39]. OH-PLIF allows for a greater resolution of the flame edge dynamics compared to CH* chemiluminescence, which is a line of sight technique.

Data processing

An Abel transform is applied to the raw CH* chemiluminescence images to extract a 2D projection of the flame from the line-of-sight data [40]. Due to the tonal nature of instability, CH* chemiluminescence images are processed in the frequency domain to isolate the fluctuations at the dominant instability frequency. Additional analysis of the instability was provided by applying a Rayleigh index calculation on the time series to show which regions in the flame are responsible for the driving and damping of thermoacoustic oscillations. This calculation is described in Equation (2), where heat-release fluctuation amplitude, q', is determined by CH* image intensity (in units of counts), and the pressure times series, P', is down-sampled to 4 kHz to match the chemiluminescence image framerate. Due to the compact shape of the flame relative to the acoustic wavelength, it is assumed that the pressure fluctuations measured on the nozzle centerbody can be applied equally over the whole flame.

$$RI = \frac{1}{t_f - t_i}\int_{t_i}^{t_f} P'q'dt \qquad (2)$$

OH-PLIF images are modified from their raw state by applying a sheet correction to account for axial variations in the laser intensity profile. A Gaussian smoothing function and bilateral noise reduction are then applied to further improve image quality before the images are binarized using a modified Otsu's method [41]. An edge tracking algorithm is used on the binarized PLIF images to determine the location of the left and right flame edges in each frame. The instantaneous lateral position of the flame edge is compared to the time-averaged position to determine the edge displacement fluctuation, L', as seen in Figure 2. These values are used to quantify flame edge

dynamics in the region near the combustor inlet as the lateral displacement fluctuation is a good measure for local heat release oscillations and transverse instability amplitude.

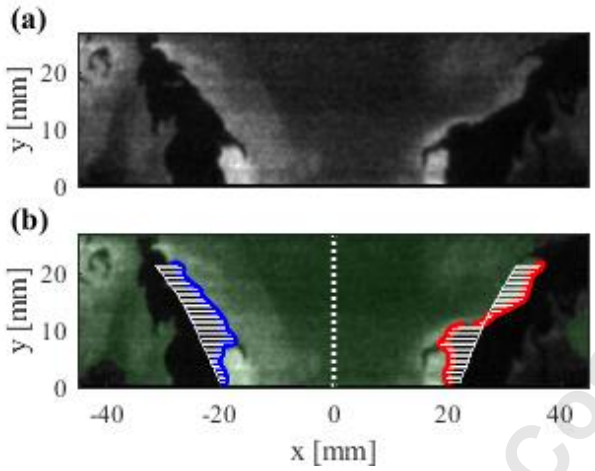

Figure 2: (a) Unprocessed and (b) binarized LIF images with detected edges (blue and red), time averaged edge locations (white), and instantaneous L' magnitudes (white horizontal)

The relationship between L' and heat release rate fluctuation in velocity-coupled flames was shown previously by Shanbhogue *et al.* [41] in their study of bluff-body stabilized flames. As the major contribution to heat release rate fluctuations from a premixed flame is through fluctuations in flame area, tracking the displacement of the flame in a planar measurement can be directly related to the area fluctuation, particularly in an axisymmetric flame. Comparisons between experimental measurements and theoretical calculations of flame heat release rate dynamics from level-set calculations by Shin *et al.* [42] showed the utility of this method for capturing flame dynamics. The inlet region of the combustor was chosen for analysis to capture the initial disturbances that develop into large-scale thermoacoustic oscillations.

RESULTS AND DISCUSSION

Instability characteristics

Acoustic oscillation intensity is quantified using the RMS of the pressure fluctuation amplitude, P'_{RMS}, which is calculated in a +/- 10 Hz band centered at the instability frequency. The frequencies of the instability are between 505 and 515 Hz, which is the quarter-wave mode of the combustor. P'_{RMS} values are calculated using two seconds of pressure data from before and after the transient to capture both the stable and unstable pressure fluctuation amplitudes. Boxplots of these values for varying degrees of premixedness are shown for both transient directions in Figure 3, with each plot representing data from 10 repeated cases. Pressure is reported in Pascals on the vertical axis and the horizontal axis shows the global equivalence ratio at each part of the transient tests. In these plots, the horizontal red lines represent the median value of the data set, the blue boxes mark the inner-quartile range about the median, horizontal black lines mark minimum and maximum values, red crosses show outliers, diagonal lines connecting adjacent boxplots represent an equivalence ratio transient in either the positive or negative direction, and the dashed horizontal line at 500 Pa marks the threshold for instability.

Journal of Engineering for Gas Turbines and Power. Received August 27, 2020;
Accepted manuscript posted January 4, 2021. doi:10.1115/1.4049486

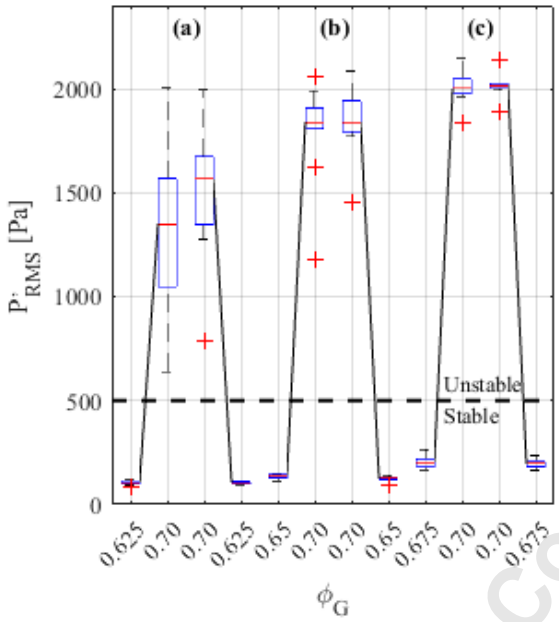

Figure 3: Boxplot diagrams of *P'* showing onset and decay of instability for (a) $\tilde{p}$ = 0.90, (b) $\tilde{p}$ = 0.93, and (c) $\tilde{p}$ = 0.96

For each test case, the premixedness during the unstable operation matches the values in Table 1 and is equal for both onset and decay transient cases with the same stable equivalence ratio. Figure 3 shows that as the degree of premixedness increases, so too does the instability amplitude. Differences in instability amplitude between the different premixing levels are statistically significant because the inner-quartile ranges for each case do not overlap. The median unstable P'_{RMS} for the most premixed case is ~48% larger than the median of the least premixed case. It is also shown that there is little difference between the forward and backward transient cases, so all further analysis combines them in reporting results.

Time-averaged flame shape

The structure of unstable flames is visualized using time-averaged CH* chemiluminescence images; the flame is a centerbody-stabilized V-flame. A comparison of the flame structures with

Journal of Engineering for Gas Turbines and Power. Received August 27, 2020;
Accepted manuscript posted January 4, 2021. doi:10.1115/1.4049486

varying degree of premixedness is shown in Figure 4. The top three images show the Abel-transformed, time-averaged images for the three levels of premixing. Three horizontal cross sections at different downstream distances of the flame are compared and the plots of the average CH* chemiluminescence intensity for each are shown in terms of count data from the camera. Figure 4 shows that near the base of the flame at Line 3, the chemiluminescence intensity slightly increases with the degree of premixedness. At Line 2, all cases show equal intensity, but farther downstream at Line 1, the least premixed case shows the most intense chemiluminescence by a small amount. These findings suggest that increasing the degree of premixedness results in a modestly more compact flame, but the general shape of the flame brush remains consistent. This compactness results in more flame penetration into the corner recirculation zone, which is an important mechanism for stabilizing the flame. As this is a time-averaged image, the further penetration into the corner recirculation zone may also indicate larger flame oscillations in that region as a result of thermoacoustic instability.

Flame fluctuations

Filtering the chemiluminescence data in the frequency domain provides another way to characterize the unsteady flame dynamics. Image data can be extracted at the dominant instability frequency, phase averaged, and integrated over the whole flame to provide a measure of CH* fluctuation intensity, measured in counts of chemiluminescence activity per Hz. The relationship between these fluctuation intensities with the previously described P'_{RMS} values can be seen in Figure 5. This plot shows a positive relationship between the intensity of pressure and CH* chemiluminescence fluctuations. Additionally, the image fluctuation intensity increases with the

degree of premixedness. This relationship is not perfect as there are several cases where the distributions of similar tests overlap, but a positive trend is still generally visible.

When normalized with the time-averaged CH* values, the CH* fluctuation images from the previous analysis show the distribution of heat release rates within the combustor. Raleigh Index calculations are used to determine where fluctuations in pressure and heat release are in phase. Both the absolute valued and normalized distributions of these index images are shown for flames with varying degrees of premixedness in Figure 6. Normalization is done with the maximum pixel intensity in each image to highlight the differences in coherent structure geometry for each flame. Positive Raleigh index values mark regions where thermoacoustic instability is being driven and negative values show regions of damping. The absolute-valued plots in Figure 6 show that the magnitude of both driving and damping of the instability increase with the degree of premixedness. Normalized images in Figure 6 show that changes in the coherent structure are most significant near the corner recirculation zone of the combustor where vortex rollup is typically observed. This region of high intensity driving grows significantly in size between the three degrees of premixedness to form a lobe shape in the most premixed case.

Journal of Engineering for Gas Turbines and Power. Received August 27, 2020;
Accepted manuscript posted January 4, 2021. doi:10.1115/1.4049486

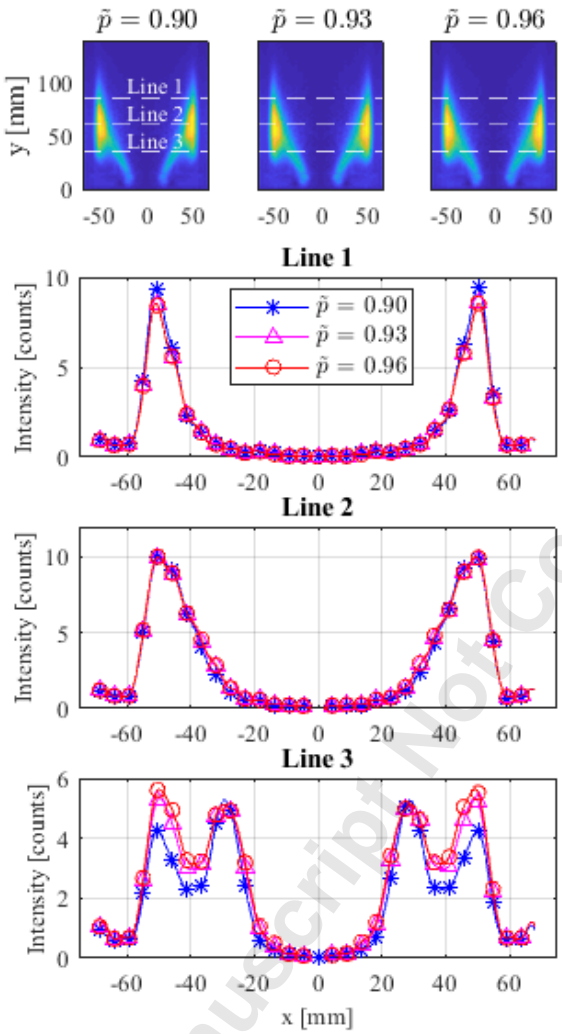

Figure 4: Time-averaged CH* chemiluminescence distribution at three downstream distances for three degrees of premixedness

Journal of Engineering for Gas Turbines and Power. Received August 27, 2020;
Accepted manuscript posted January 4, 2021. doi:10.1115/1.4049486

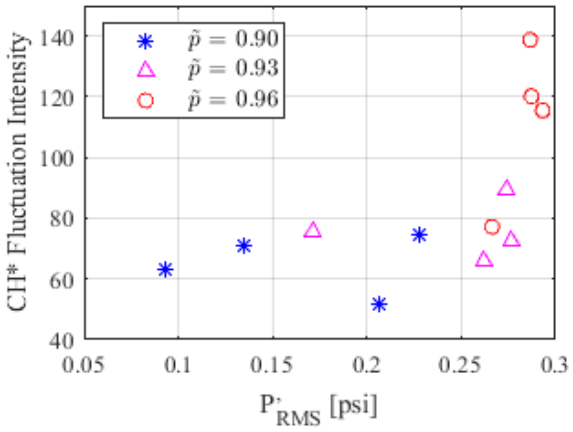

Figure 5: Chemiluminescence phase-averaged fluctuation intensity vs. pressure fluctuation intensity

Integrating the Rayleigh Index values over a specific region of the flame shows the net contribution of that area to the unstable dynamics and integrating them over the entire flame gives a sense of the net driving or damping in the system. Radially correcting the images by multiplying the count values with their offset from the radial centerline provides a more realistic measure of damping or driving from the integrated value assuming that the time-averaged flame is axisymmetric. A plot of the integrated values over the pressure fluctuation amplitudes for both the corner region and the entire flame are shown in Figure 7. The values are positive for each degree of premixedness, resulting in a net driving of instability in all cases.

The linear relationship between Rayleigh Index value and pressure fluctuation amplitude is to be expected in unstable systems. However, the differences in distribution between the degrees of premixedness shows a positive trend, which resembles the previously discussed phase-averaged fluctuation intensity in Figure 5. The comparison between the magnitude of the Rayleigh Index over the whole flame and in the corner region shows that the average values in the corner are ~2x greater than the system wide average. This dominance of the corner recirculation zone suggests that the vortex-driven dynamics in the corner region are largely responsible for determining the

instability characteristics in the system and that the relative importance of this region remains consistent for each degree of premixedness.

Further, the shape of the integrated Rayleigh Index trends with combustor pressure fluctuation intensity is notable. The Rayleigh Index integrated over the entire image increases linearly with pressure fluctuation amplitude, which is reasonable given that the pressure fluctuations are driving the heat release rate fluctuations and also the Rayleigh Index is a function of the pressure fluctuations. However, the Rayleigh Index integrated over the corner region of the flame increases at a higher slope with higher levels of premixing, indicating that the amount of driving in that region and relative importance to the overall instability feedback loop increases with premixing.

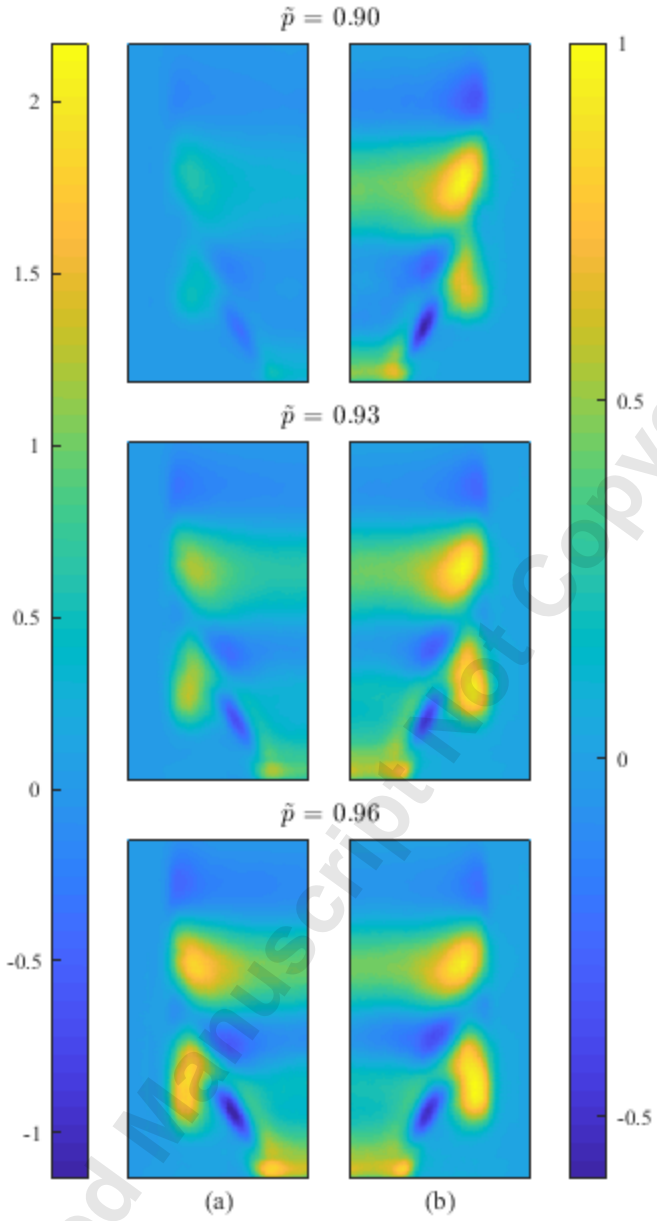

Figure 6: (a) absolute value and (b) normalized Rayleigh index images for three degrees of premixedness

Flame edge tracking

CH* chemiluminescence images are a useful tool for tracking large-scale structures and heat release dynamics. However, chemiluminescence does not provide high spatial resolution of flame dynamics and so OH-PLIF was employed to analyze local flame edge dynamics. Quantification of

Journal of Engineering for Gas Turbines and Power. Received August 27, 2020;
Accepted manuscript posted January 4, 2021. doi:10.1115/1.4049486

flame edge displacement is done by tracking the local flame edge oscillation, L', over a range of downstream distances. In this analysis we want to understand whether the degree of premixedness drives differences in local flame dynamics, given the differences seen in the Rayleigh Index in the corner recirculation zone near the base of the flame.

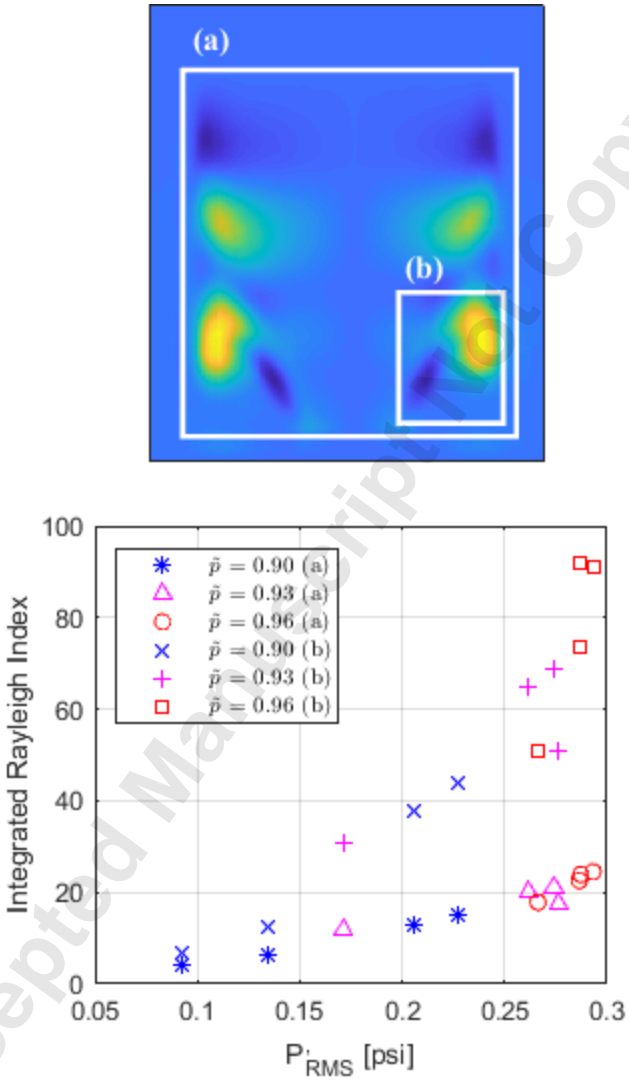

Figure 7: Rayleigh index integrated over (a) entire flame and (b) corner region

Using spectral analysis and analyzing the data at the peak frequency isolates the tonal behavior of the edge displacement and provides phase information for both the left and right flame edges.

The difference in phase between the left and right branches, $\Delta\varphi$, is useful in describing the dynamics of the flame branches and is plotted along with L'_{RMS} as a function of downstream distance in Figure 8. Analysis of the L'_{RMS} plot shows that the magnitude of fluctuations in every case increases as a function of downstream distance, which makes sense given that the flame is anchored to the centerbody at its base and its range of motion increases with downstream distance. Comparing the edge fluctuation magnitudes for each test case shows relatively similar behavior for all values of $\tilde{p}$ near the nozzle but further downstream the higher degrees of premixedness begin to deviate from the rest with slightly larger L'_{RMS} magnitudes. This finding is congruent with the results from the Rayleigh Index analysis, as the stronger flame fluctuations downstream near the corner recirculation zone drive higher amplitude thermoacoustic oscillation.

In the plot of phase difference, a $\Delta\varphi$ of π radians between the left and right branches suggests coherence in the flame structure in the form of ring vortex shedding at the exit of the swirling jet. As the magnitude of the phase difference deviates from π radians, the left and right branches of the flame lose coherence, begin to cancel each other's oscillations, and damp the instability. The phase difference plot in Figure 8b shows that all phase differentials are within 6% of π for the entirety of the PLIF window suggesting a strong coherence in all cases. All of the plots have a similar shape that begins slightly below the value of π. They then increase in magnitude until they exceed π and reach their maximum at some downstream distance before reducing once more. No clear trend can be found by the comparing the magnitudes of $\Delta\varphi$ for each value of $\tilde{p}$, suggesting that the coherence in this region is not strongly related to the premixedness of the flame.

Journal of Engineering for Gas Turbines and Power. Received August 27, 2020;
Accepted manuscript posted January 4, 2021. doi:10.1115/1.4049486

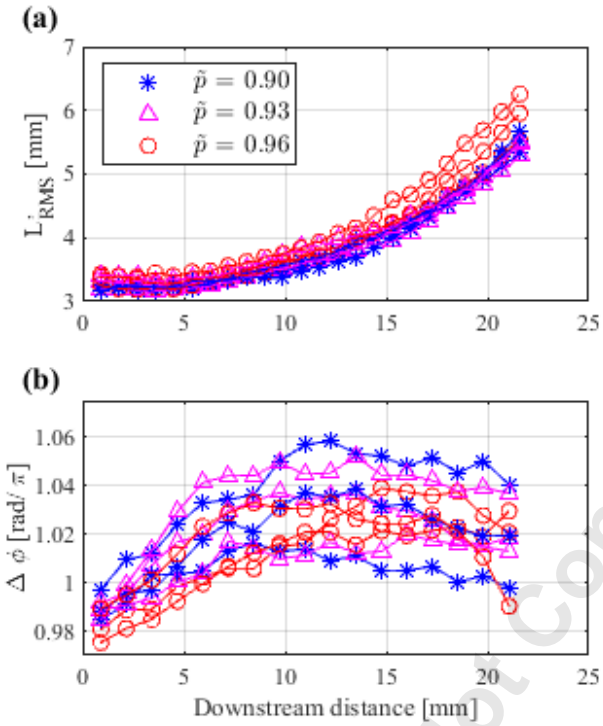

Figure 8: (a) L' and (b) $\Delta\phi$ for all test cases

DISCUSSION

The results presented show clear changes in combustion instability characteristics with the degree of premixedness. These findings can be applied to the current model self-excited instability, which states that a feedback loop forms when equivalence ratio perturbations, fluctuations in heat release, flow-field oscillations, and combustor acoustics become relatively in phase and drive instability. In the current analysis, the degree of premixedness potentially describes equivalence ratio perturbations, the CH* chemiluminescence intensity quantifies the heat release rate, edge displacement oscillations (*L'*) define the flame's response to flow field dynamics and the pressure fluctuations (*P'*) describe the acoustics.

Analysis of combustor pressure fluctuations show that the magnitude of instability increases with the degree of premixedness. CH* fluctuation analysis shows a similar correlation with the

inclusion of heat release. The changes in the instability behavior shown in the Rayleigh Index analysis suggest a shift in the phase between one or more of the dynamic oscillations leading to a change in the coherent structures. Increasing the degree of premixedness could result in a decrease to the equivalence ratio perturbation amplitude; as more fuel is provided in the "fully premixed circuit," then more of the fuel/air mixture is mixed ahead of a choke plate, which suppresses fuel perturbations. However, measurements of instantaneous pressure in the partially-premixed fuel system 0.1 m upstream of the fuel-injection location show no coherent oscillations in the fuel system during instability. This finding indicates that there are negligible equivalence ratio fluctuations during instability and so the equivalence-ratio coupling mechanism is not important in this system.

It is hypothesized that the change in the instability amplitude is driven by the change in mean flame shape due to premixing and that interaction between the coherent vortical structures in the corner region and the flame is what governs the changes in the system dynamics. This hypothesis is supported directly by the Rayleigh Index analysis, which identified the location of vortex rollup as the leading source of driving in the unstable system and found that the magnitude of this driving varies with premixedness. As the level of premixedness increases, more of the flame is stabilized in the corner recirculation zone, as shown in Figure 4. Analysis of flame edge oscillations also provide validation for this as they show that there is very little change in edge dynamics near the inlet of the combustor, but that the flame fluctuation near the wall-impingement region of the highest premixedness case shows higher levels of fluctuation.

The change in the flame shape due to the level of premixedness is likely a result of the partially-premixed fuel injection location. This fuel is injected through holes located on the upstream surface of the swirler vanes, which encourages mixing between the fuel and air as the flow passes through

the swirler vanes. However, the distance between the fuel-injection location and the base of the flame is only 0.1 m, meaning mixing is likely not perfect. Recent experiments at the same inlet temperature and flow rate in this study but with an equivalence ratio of 0.65 (a stable condition) were conducted with both fully-premixed and entirely technically-premixed fuel injection. Results from these stable flames show that the flame angle widens by 2° in the technically premixed condition, which is not a significant difference given the overall flame angle of the fully premixed case is 28°. The technically premixed configuration has stronger chemiluminescence emission near the anchoring point of the flame at the bluff body than does the fully premixed flame, whereas the fully premixed flame has stronger chemiluminescence emission near the end of the recirculation zone. Given that the main mechanism of heat release rate oscillation is vortex shedding in the corner recirculation zone, the bias of heat release in the fully premixed case towards the recirculation zone is likely the reason that the instability driving magnitude, given by the Rayleigh index in this study, increases with the degree of premixedness. These results show that even subtle changes to the fuel/air mixing process can result in flame shape changes that alter the thermoacoustic feedback cycle.

CONCLUSIONS

This work considered the effects of the degree of premixedness on self-excited thermoacoustic instability in a single-nozzle, swirl-stabilized, gas turbine combustor. It was found that under the conditions described, that increasing the degree of premixedness of the fuel/air mixture at the inlet increased the amplitude of self-excited instability. The source of the changes was found to be at the point of vortex rollup, where it is hypothesized that the change in time-averaged flame shape

with premixing changes the magnitude of heat release rate oscillations in certain parts of the flame during instability.

One potential implication of this is that increasing the degree of premixedness may not always increase instability amplitude, as the specific relationships between the thermoacoustic oscillations vary from combustor to combustor. More detailed characterization of fuel-air mixing and distributions, as well as their effect on the flame, is necessary for better understanding. Another implication may be that this finding may not be applicable in the design of multi-nozzle combustors due to the presence of flame interactions, which dominate the shape of the flame and hence the impact that the mechanism of instability has on flame heat release rate oscillations. Future work may be to perform a similar study on a multi-nozzle combustor to test the impact of varying premixedness in more practical combustor designs.

ACKNOWLEDGEMENTS

This work was funded by the US Department of Energy University Turbine Systems Research Program under grant DE-FE0025495 with program monitor Mark Freeman. The authors thank Ankit Tyagi, Xiaoling Chen, and Wyatt Culler for assistance in data processing

REFERENCES

[1] Y. Huang and V. Yang, “Bifurcation of flame structure in a lean-premixed swirl-stabilized combustor: Transition from stable to unstable flame,” *Combust. Flame*, vol. 136, no. 3, pp. 383–389, 2004.

[2] T. C. Lieuwen and V. Yang, “Combustion Instabilities in Gas Turbine Engines: Operational Experience, Fundamental Mechanisms, and Modeling,” *Prog. Astronaut. Aeronaut.*, 2010.

[3] T. C. Lieuwen, “Experimental Investigation of Limit-Cycle Oscillations in an Unstable Gas

Turbine Combustor," *J. Propuls. Power*, vol. 18, no. 1, pp. 61–67, 2002.

[4] D. Durox *et al.*, "Flame Dynamics of a Variable Swirl Number System and Instability Control," *Combust. Flame*, vol. 160, no. 9, pp. 1729–1742, 2013.

[5] A. J. De Rosa, S. J. Peluso, B. D. Quay, and D. A. Santavicca, "The Effect of Confinement on the Structure and Dynamic Response of Lean-Premixed, Swirl-Stabilized Flames," *J. Eng. Gas Turbines Power*, vol. 138, no. 6, p. 061507, 2015.

[6] A. J. De Rosa, S. J. Peluso, B. D. Quay, and D. A. Santavicca, "Lean-Premixed, Swirl-Stabilized Flame Response: Flame Structure and Response as a Function of Confinement," *J. Eng. Gas Turbines Power*, vol. 140, no. 3, p. 031504, 2017.

[7] T. Lieuwen and B. T. Zinn, "The Role of Equivalence Ratio Oscillations in Driving Combustion Instabilities in Low NOx Gas Turbines," *Symp. Combust.*, vol. 27, no. 2, pp. 1809–1816, 1998.

[8] J. H. Cho and T. Lieuwen, "Laminar Premixed Flame Response to Equivalence Ratio Oscillations," *Combust. Flame*, vol. 140, no. 1–2, pp. 116–129, 2005.

[9] Shreekrishna, S. Hemchandra, and T. Lieuwen, "Premixed Flame Response to Equivalence Ratio Perturbations," *Combust. Theory Model.*, vol. 14, no. 5, pp. 681–714, 2010.

[10] J. Samarasinghe, W. Culler, B. D. Quay, D. Santavicca, and J. O'Connor, "The Effect of Fuel Staging on the Structure and Instability Characteristics of Swirl-Stabilized Flames in a Lean Premixed Multi-Nozzle Can Combustor," *J. Tribol.*, vol. 139, no. 12, 2017.

[11] W. Culler, X. Chen, J. Samarasinghe, S. Peluso, D. Santavicca, and J. O'Connor, "The Effect of Variable Fuel Staging Transients on Self-Excited Instabilities in a Multiple-Nozzle Combustor," *Combust. Flame*, vol. 194, pp. 472–484, 2018.

[12] W. Culler, X. Chen, S. Peluso, D. Santavicca, and D. Noble, "Comparison of Center Nozzle

Staging To Outer Nozzle Staging in a Multi-Flame Combustor," *Proc. ASME Turbo Expo*, 2018.

[13] O. Sekulich, W. Culler, and J. O'Connor, "An Investigation of the Effects of Fuel Staging on Flame Structure in a Gas Turbine Model Combustor," *Proc. ASME Turbo Expo*, vol. 1 B, pp. 1–9, 2018.

[14] J. Cohen, G. Hagen, A. Banaszuk, and S. Becz, "Attenuation Of Combustor Pressure Oscillations Using Symmetry Breaking," *49th AIAA Aerosp. Sci. Meet.*, 2011.

[15] N. Noiray, M. Bothien, and B. Schuermans, "Investigation of azimuthal staging concepts in annular gas turbines," *Combust. Theory Model.*, vol. 15, no. 5, pp. 585–606, 2011.

[16] N. Noiray and B. Schuermans, "On the dynamic nature of azimuthal thermoacoustic modes in annular gas turbine combustion chambers," *Proc. R. Soc. A 469*, 2012.

[17] G. Ghirardo and M. P. Juniper, "Azimuthal instabilities in annular combustors : standing and spinning modes," *Proc. R. Soc. A 469*, 2013.

[18] T. Sattelmayer, "Influence of the Combustor Aerodynamics on Combustion Instabilities From Equivalence Ratio Fluctuations," *J. Eng. Gas Turbines Power*, vol. 125, no. 1, p. 11, 2003.

[19] S. Ducruix, T. Schuller, D. Durox, and S. Candel, "Combustion Dynamics and Instabilities: Elementary Coupling and Driving Mechanisms," *J. Propuls. Power*, vol. 19, no. 5, pp. 722–734, 2003.

[20] P. Palies, D. Durox, T. Schuller, and S. Candel, "The Combined Dynamics of Swirler and Turbulent Premixed Swirling Flames," *Combust. Flame*, vol. 157, no. 9, pp. 1698–1717, 2010.

[21] X. Chen, W. Culler, S. Peluso, D. Santavicca, and J. O'Connor, "Effects of the equivalence

ratio transient durations on selfexcited combustion instability time scales in a single nozzle combustor," *2018 Spring Tech. Meet. East. States Sect. Combust. Institute, ESSCI 2018*, vol. 2018–March, pp. 1–8, 2018.

[22] K. Venkatesan, A. Cross, C. Yoon, F. Han, and S. Bethke, "Heavy Duty Gas Turbine Combustion Dynamics Study Using a Two-Can Combustion System," *Proc. ASME Turbo Expo*, 2019.

[23] T. Lieuwen, H. Torres, C. Johnson, and B. T. Zinn, "A Mechanism of Combustion Instability in Lean Premixed Gas Turbine Combustors," *J. Eng. Gas Turbines Power*, vol. 123, no. 1, p. 182, 2001.

[24] X. Chen, W. Culler, S. Peluso, D. Santavicca, and J. O. Connor, "Comparison of Equivalence Ratio Transients on Combustion Instability in Single-Nozzle and Multi-Nozzle Combustors," *Proc. ASME Turbo Expo*, pp. 1–10, 2018.

[25] J. Kariuki, N. Worth, J. Dawson, and E. Mastorakos, "Visualisation of blow-off events of two interacting turbulent premixed flames," *AIAA Aerosp. Sci. Meet. Incl. New Horizons Forum Aerosp. Expo.*, no. January, 2013.

[26] B. Dolan, R. V. Gomez, and E. Gutmark, "Optical Measurements of Interacting Lean Direct Injection Fuel," *Proc. ASME Turbo Expo*, 2015.

[27] D. Fanaca, P. R. Alemela, C. Hirsch, and T. Sattelmayer, "Comparison of the Flow Field of a Swirl Stabilized Premixed Burner in an Annular and a Single Burner Combustion Chamber," *J. Eng. Gas Turbines Power*, vol. 132, no. 7, p. 071502, 2010.

[28] M. Szedlmayer, "An Experimental Study of the Velocity Forced Flame Response of a Lean premixed multi-Nozzle Can Combustor for Gas Turbines," no. August, 2013.

[29] T. Smith, B. Emerson, I. Chterev, D. R. Noble, and T. Lieuwen, "Flow Dynamics in Single

and Multi - Nozzle Swirl Flames," *Proc. ASME Turbo Expo*, 2016.

[30] T. E. Smith, I. P. Chterev, B. L. Emerson, and D. R. Noble, "Comparison of Single- and Multinozzle Reacting Swirl Flow Dynamics," *J. Propuls. Power*, vol. 34, no. 2, 2018.

[31] J. Samarasinghe, S. Peluso, M. Szedlmayer, A. De Rosa, B. Quay, and D. Santavicca, "Three-Dimensional Chemiluminescence Imaging of Unforced and Forced Swirl-Stabilized Flames in a Lean Premixed Multi-Nozzle Can Combustor," *J. Eng. Gas Turbines Power*, vol. 135, no. 10, 2013.

[32] P. Orwannukul, "An Experimental Study of Flame Response in a Technically- Premixed Multi-Nozzle Gas Turbine Combustor," no. August, 2014.

[33] A. M. Kypraiou, P. M. Allison, A. Giusti, and E. Mastorakos, "Response of Flames with Different Degrees of Premixedness to Acoustic Oscillations," *Combust. Sci. Technol.*, vol. 190, no. 8, pp. 1–16, 2018.

[34] A. M. Kypraiou, A. Giusti, P. M. Allison, and E. Mastorakos, "Dynamics of Acoustically Forced Non-Premixed Flames Close to Blow-off," *Exp. Therm. Fluid Sci.*, vol. 95, no. January, pp. 81–87, 2018.

[35] J. Samarasinghe, W. Culler, D. A. Santavicca, and J. O. Connor, "The Effect of Fuel Staging on the Structure and Instability Characteristics of Swirl-Stabilized Flames in a Lean Premixed Multinozzle Can Combustor," *J. Eng. Gas Turbines Power*, vol. 139, no. December, pp. 1–10, 2017.

[36] A. D. Pierce, *Acoustics: An Introduction to Its Physical Principles and Applications*, Third Edit. Acoustical Society of America, 2019.

[37] N. A. Worth and J. R. Dawson, "Cinematographic OH-PLIF Measurements of Two Interacting Turbulent Premixed Flames With and Without Acoustic Forcing," *Combust.*

Flame, vol. 159, no. 3, pp. 1109–1126, 2012.

[38] N. A. Worth and J. R. Dawson, "Tomographic Reconstruction of OH* Chemiluminescence in Two Interacting Turbulent Flames," *Meas. Sci. Technol.*, vol. 24, no. 2, 2013.

[39] W. Culler, "An Experimental Investigation of Fuel Staging in a Model Gas Turbine Combustor," 2018.

[40] Z.-G. Yuan, "The Filtered Abel Transform and Its Application in Combustion Diagnostics," no. March, p. 16, 2003.

[41] S. Shanbhogue, D. H. Shin, S. Hemchandra, D. Plaks, and T. Lieuwen, "Flame sheet dynamics of bluff-body stabilized flames during longitudinal acoustic forcing," *Proc. Combust. Inst.*, vol. 32 II, no. 2, pp. 1787–1794, 2009.

[42] D. Shin, D. V Plaks, T. Lieuwen, U. M. Mondragon, C. T. Brown, and V. G. Mcdonell, "Dynamics of a Longitudinally Forced , Bluff Body Stabilized Flame," *J. Propuls. Power*, vol. 27, no. 1, 2011.